Journal of Alloys and Compounds 836 (2020) 155472

Contents lists available at ScienceDirect

Journal of Alloys and Compounds

journal homepage: http://www.elsevier.com/locate/jalcom

The effect of stress distribution in the bulk of a microwire on the magnetization processes

O.I. Aksenov [a, *], A.A. Fuks [a, b], A.S. Aronin [a, b]

[a] Institute of Solid State Physics, RAS, Chernogolovka, Russia
[b] National Research University Higher School of Economics, Moscow, Russia

ARTICLE INFO

Article history:
Received 10 March 2020
Received in revised form
30 April 2020
Accepted 2 May 2020
Available online 11 May 2020

Keywords:
Microwires
Amorphous materials
Stress tensor
Stress distribution
Magnetic properties
Adhesion

ABSTRACT

The effect of tensile stresses on the magnetic properties of amorphous microwires with positive magnetostriction has been studied. It has been determined that the experimental dependence of coercivity on the tensile stresses is reversible and consists of linear and square root parts. The evolution of an average stress level in the “core” and surface domain layer has been theoretically estimated depending on the external tensile stress. The value of internal stress level may vary from 150 to 600 MPa in “core” for microwires with different ratio of amorphous metallic nucleus diameter to thickness of glass shell. Crucial differences of tension of glass-coated and uncoated microwires have been investigated. The analysis of these differences with relation to effect under tension has been performed.

1. Introduction

High magnetic permeability, low magnetization losses and other soft magnetic material properties are characteristic of amorphous ferromagnetics. This makes them an attractive object for investigation and further application. In recent years, considerable attention has been paid to the study of the optimization of the magnetic parameters of microwires. Work is also underway on the application of amorphous microwires as magnetic sensors [1–3]. An isotropic atomic structure and the absence of crystalline order cause the main effect of magnetoelastic anisotropy on their magnetic properties. Hence, the study of the magnetic properties of amorphous ferromagnetics depending on the stress state is of great interest [4,5]. In particular, there is considerable interest in the investigation of glass-coated amorphous microwires produced by rapid melt quenching. The anisotropic magnetic structure of a microwire consists of central part domains (“core”) with magnetic moment orientation along the wire axis and of a surface ring domain layer with magnetic moment orientation depending on the sign of magnetostriction λ_s (positive or negative). The orientation of magnetic moment of surface domains is radial for microwires with positive magnetostriction [6,7]. The anisotropy of a surface domain layer and the “core” is significantly different. Furthermore, it should be noted that the coercivity of a microwire is determined by the magnetization reversal of the “core”. This structure is caused mainly by a non-uniform tensor of internal stress arising in a material as a result of quenching, reeling, and cooling-down (due to the difference in the thermal expansion coefficients of the glass shell and amorphous metallic nucleus). The correlation between magnetic properties and stress state of microwires [8–13] is combined with their compactness, flexibility, isolation from the environment by the glass shell. Based on the foregoing, magnetic properties of microwires such as giant magneto-impedance effect, single domain wall propagation, etc [14–19] are of great interest to application. The glass shell is especially important for biocompatible applications of microwires. It eliminates foreign body rejection and thus enables using microwires in living tissue. This and many other reasons explain special attractiveness of application of glass-coated microwires.

Over the last twenty years, considerable attention is being given to the study of the magnetic properties of amorphous microwires depending on the change in their stress state by annealing, twisting, tension, etc [20–22,23]. There is theoretical approach to describe non-uniform stress distribution in microwires [24]. However, experimental methods of measurements of stress level in

* Corresponding author.
E-mail address: oleg_aksenov@inbox.ru (O.I. Aksenov).

https://doi.org/10.1016/j.jallcom.2020.155472
0925-8388/

microwire are practically non-existent. The work [8] especially deserves mention. In Ref. [8], the value of internal stress level in the bulk of glass-coated microwires is measured, by magnetic hysteresis loops analysis.

Nowadays, there are no works which describe the interaction between the glass shell and the amorphous metallic nucleus under tension and magnetization. Meanwhile, such investigation is interesting in respect to the prospects of glass-coated microwires application.

This work aims to study the effect of tension on the magnetic properties of glass-coated microwires with positive magnetostriction.

2. Experimental procedures

Glass-coated amorphous microwires with $Fe_{73.8}Cu_1Nb_{2.1}B_{9.1}Si_{13}$ composition and different d/D ratios (where d is the amorphous metallic nucleus diameter, and D is the total diameter including the glass shell) are investigated.

All the microwires under study are produced by the Taylor-Ulitovsky method. The saturation magnetostriction λ_s of the microwires under study is $39x10^{-6}$ [22]. The microwires under study are listed in Table 1.

Saturation and remanent magnetization are measured by vibrating sample magnetometry.

The coercivity dependence on the external tensile stress of the microwires is measured by pick-up coil magnetometry under tension in situ. The tension is carried out up to 2 GPa (close to the tensile strength limit of the material) [25]. Measuring accuracy of coercivity is 0.5 Oe. Measuring accuracy of tension stress is 10 MPa. The complete description of measurement scheme is presented in Ref. 24.

The geometrical parameters of the microwires under study (thickness of the glass shell, diameter of the amorphous metallic nucleus) are determined using a Supra 50vp scanning electron microscope.

The glass shell is removed by chemical etching for the preparation of uncoated microwires.

The structure of the microwires is studied by X-ray diffraction on SIEMENS D-500 diffractometer with using of Co K_α radiation.

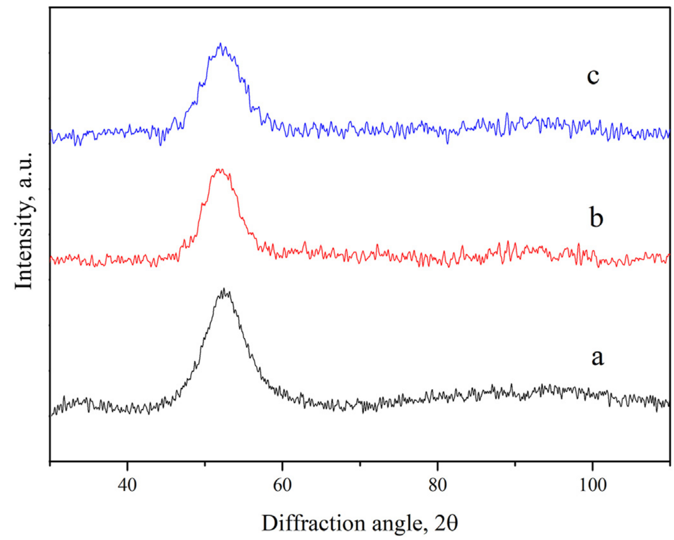

Fig. 1. X-ray diffraction patterns of microwires with (a) d/D = 0.76, (b) d/D = 0.7 and (c) d/D = 0.48.

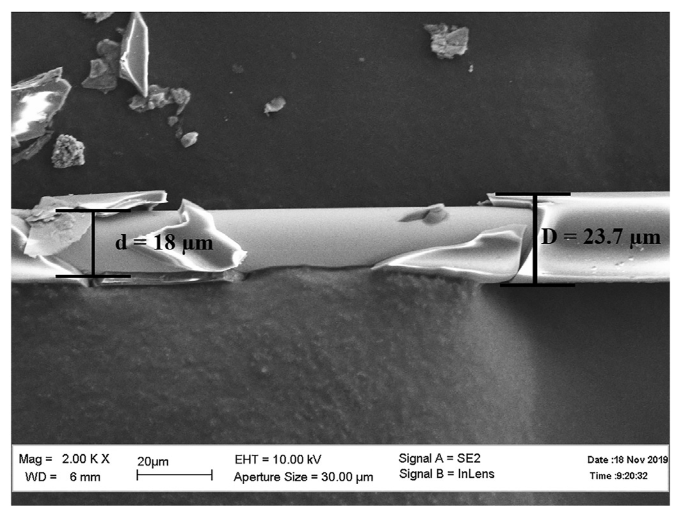

Fig. 2. SEM image of microwire with d/D = 0.76.

3. Results and discussion

Fig. 1 shows X-ray diffraction patterns of the microwires under study.

All the microwires under study are amorphous. It is confirmed by the results of X-ray diffraction analysis due to the presence of diffusion halo and the absence of crystalline peaks.

Figs. 2–4 show scanning electron microscopy (SEM) images of microwires under study.

Fig. 5 demonstrates a typical curve of coercivity dependence on the tension in-situ for a glass-coated microwire.

For glass-coated microwires, the value of tensile stress applied to the amorphous metallic nucleus is calculated by the expression:

$$\sigma_t = F / (S_a + S_g E_g / E_a) \quad (1)$$

where σ_t is the tension stress applied to the amorphous metallic nucleus, F is the applied force, S_a is the sectional area of the amorphous metallic nucleus, S_g is the sectional area of the glass shell, E_g and E_a are the Young's moduli of the glass shell and amorphous metallic nucleus, respectively [26,27].

It is accepted that both the switching field and the coercivity of amorphous microwires are proportional to the energy necessary to form a domain wall in the "core" which occurs under bistable magnetization reversal of a wire. Based on Ref. 20, coercivity is

Table 1
List of the microwires under study.

Composition	Metallic nucleus diameter, d (µm)	Total diameter, D (µm)	d/D ratio
$Fe_{73.8}Cu_1Nb_{2.1}B_{9.1}Si_{13}$	18	23.7	0.76
	16.8	23.7	0.7
	11.4	24	0.48

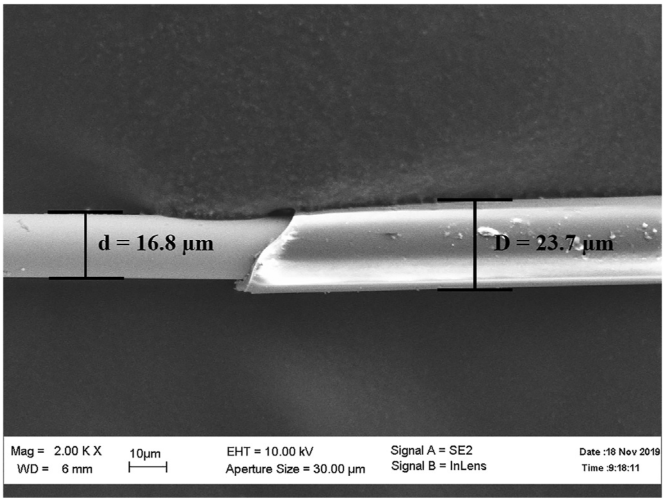

Fig. 3. SEM image of microwire with d/D = 0.7.

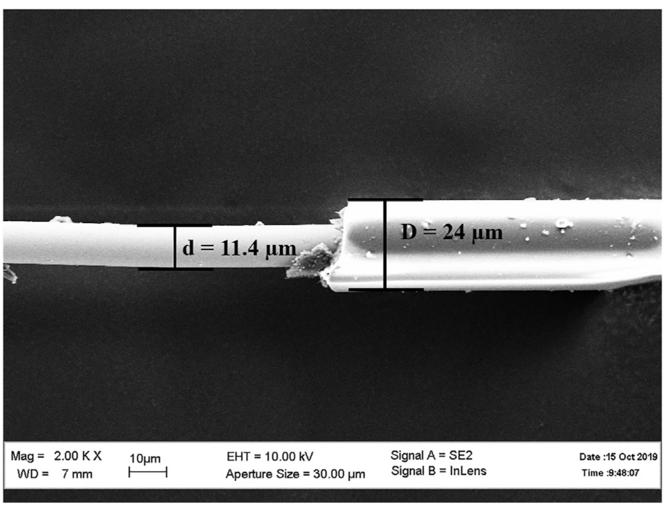

Fig. 4. SEM image of microwire with d/D = 0.48.

calculated as the ratio:

$$H_C \sim \left[A\left(\frac{3}{2}\right)\lambda_s(\sigma_t + \sigma_i)\right]^{1/2} \Big/ \cos\alpha \quad (2)$$

where A is the exchange energy constant, λ_s is the saturation magnetostriction constant, σ_t is the applied tension stress value, σ_i is the internal stress value, α is the angle between magnetization and a magnetic field direction. Therefore, when σ_t is greater than the internal stress value and at small angles α, coercivity is proportional to the square root of the applied tension stress [28].

Fig. 6 demonstrates curves of coercivity dependence on the external tension stress for glass-coated and uncoated microwires with different initial stress levels (different d/D ratios).

In Fig. 6, uncoated microwires are also denoted with d/D ratio to show that these wires correspond to initial glass-coated wires after glass removal (both in geometry and composition). The initial coercivity for microwires with different d/D ratios is shown in Table 2. Different d/D ratios conform to the different levels of internal stresses resulting from the manufacturing process of a microwire. This is related to the difference in the thermal

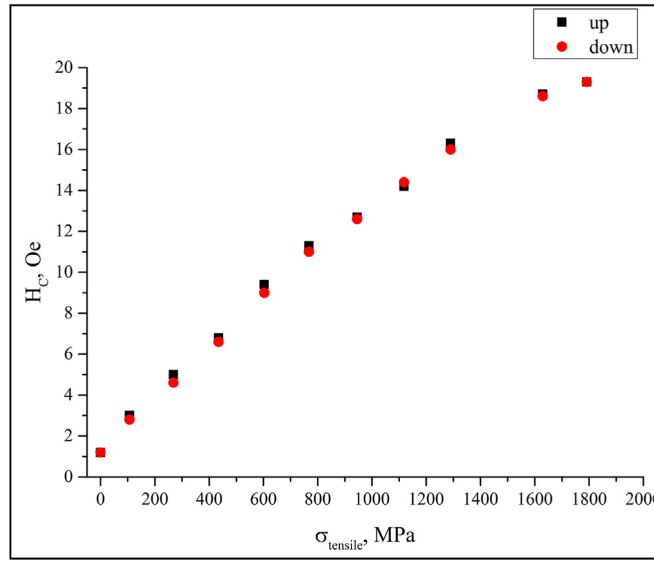

Fig. 5. Coercivity dependence on the applied tension stress under loading (up) and unloading (down) the glass-coated microwire with d/D = 0.7.

expansion coefficients of the glass shell and amorphous metallic nucleus. Less values of d/D ratio correspond to a higher stress level in the material.

The experimental points in Fig. 6 were fitted by the equation:

$$H_C = A\sigma^x \quad (3)$$

where A is the constant, σ is the value of tensile stress, x is the index of power. The results of fitting for all the microwires under study are listed in Table 3.

As one can see from Table 2, the dependence of coercivity on the stress strictly follows the root law for the uncoated microwires with the diameter d = 16.8 μm. The dependence $H_C(\sigma)$ also has the form close to the root one for the uncoated microwires with the diameter d = 18 μm. A weaker dependence of coercivity on the stress is observed for the uncoated microwires with the diameter d = 11.4 μm.

In case of glass-coated microwires the dependence is more complicated. A significant deviation from the root dependence is observed for the microwires with the ratio d/D = 0.7. Previously it was also noted in Ref. [24,28] that the coercivity dependence on the stress deviates from a root form. In that work, the function describing the coercivity dependence on the stress has the form:

$$H_C = B + \sigma^y \quad (4)$$

where B is the constant, σ is the value of tensile stress (MPa), y is the index of power.

In Ref. 28, the index of power for a microwire with the ratio d/D = 0.88 is 0.74. However, there are no specific conclusions in Ref. 28 on the reasons for this deviation.

Moreover, Fig. 6 (a) demonstrates that fitting by a power function does not agree well with the experimental points. This becomes more evident for microwires with a thicker glass shell.

It seems that for the case of glass-coated microwires there is an extended linear part of H_C (σ) dependence (up to 600–800 MPa). This increases with increase of initial stress state.

It follows there are “linear function” and “power function” working areas of a microwire. This is a significant result regarding application of microwires as stress sensors. Fig. 7 demonstrates the dependence of coercivity on the stress for the glass-coated

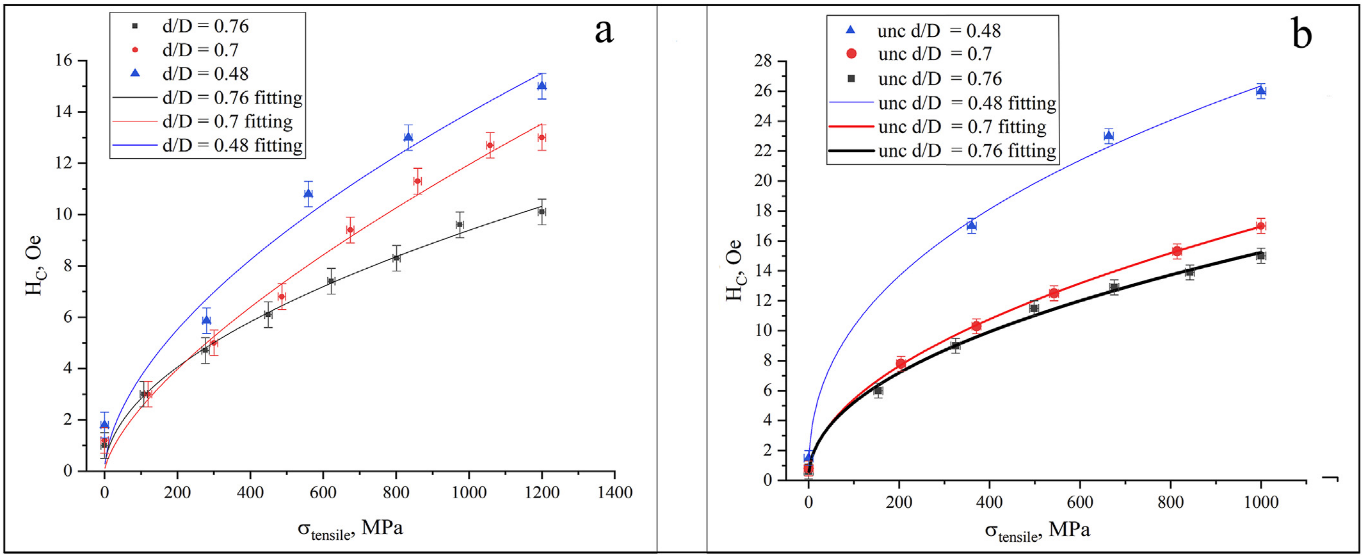

Fig. 6. Coercivity dependence on the applied tension stress for (a) glass-coated and (b) uncoated microwires.

Table 2
Initial coercivity for microwires with different d/D ratios.

d/D	Presence of the glass shell	H_C, Oe
0.48	Glass-coated	2
	Uncoated	1.5
0.7	Glass-coated	1.1
	Uncoated	0.5
0.76	Glass-coated	1
	Uncoated	0.8

Table 3
The results of fitting of the experimental points in Fig. 6.

d/D	Presence of the glass shell	A	x
0.48	Glass-coated	0.26 ± 0.16	0.58 ± 0.09
	Uncoated	1.56 ± 0.6	0.41 ± 0.06
0.7	Glass-coated	0.1 ± 0.03	0.68 ± 0.04
	Uncoated	0.55 ± 0.02	0.5 ± 0.005
0.76	Glass-coated	0.26 ± 0.03	0.58 ± 0.09
	Uncoated	0.61 ± 0.1	0.47 ± 0.02

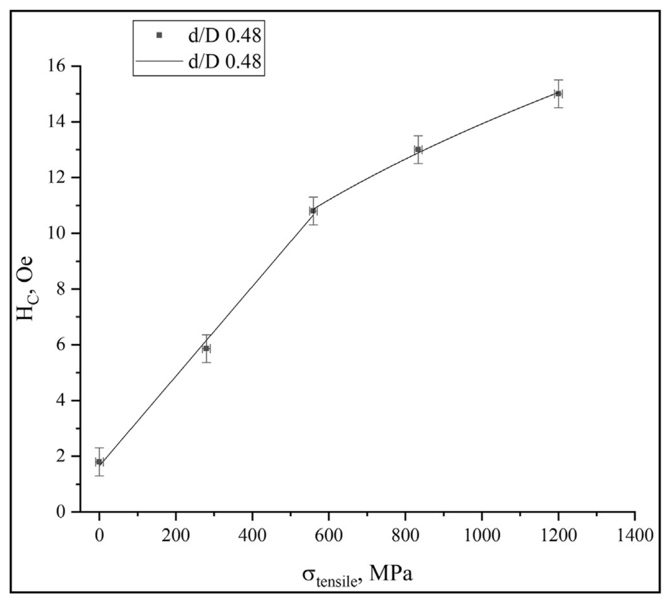

Fig. 7. Fitting of the H_C (σ) dependence in the assumption that the initial curve part is a linear function.

microwire with the ratio d/D = 0.48. Fitting in Fig. 7 was performed in the assumption that the initial part of the H_C (σ) curve (up to 600 MPa) is a linear function, and the last part is a power function.

As one can see from Fig. 7, this fitting provides better convergence with the experimental data than the result in Fig. 6 that was obtained by the fitting by the power function.

Fig. 6 shows that the rate of coercivity increase in Hc (σ) curves for uncoated microwires is higher than that for glass-coated microwires. That is, the largest increase in the internal stress is observed under the tension of uncoated microwires. At that, an increase in the coercivity of microwires with the lowest d/D ratio, and hence with the largest initial stress level, is higher than that of microwires with a higher d/D ratio. Note also that the rate of coercivity increase for microwires with the lowest diameter, and hence with the largest residual stress level due to quenching, is higher than that for microwires with a higher diameter. These effects can be explained in terms of a change in the stress state of a microwire.

Previously the stress state of glass-coated and uncoated microwires was estimated in Ref. 17. However, the theoretical estimation of the size of domain regions for the "core" and surface domain layer differs from the experimental estimation by 10–15%. The theoretical estimation should be adjusted to the real size of domain regions. This is significant for the estimation of an average stress in a microwire.

It is possible to estimate the size of domain regions by the ratio of remanent magnetization to saturation magnetization [29]:

$$R_C \Big/ R_m = (M_r/M_S)^{1/2} \tag{5}$$

where R_C is the "core" radius, R_m is the amorphous metallic nucleus radius, M_r is the remanent magnetization, M_S is the saturation magnetization.

Figs. 8 and 9 demonstrate hysteresis loops of the glass-coated and uncoated microwires under study.

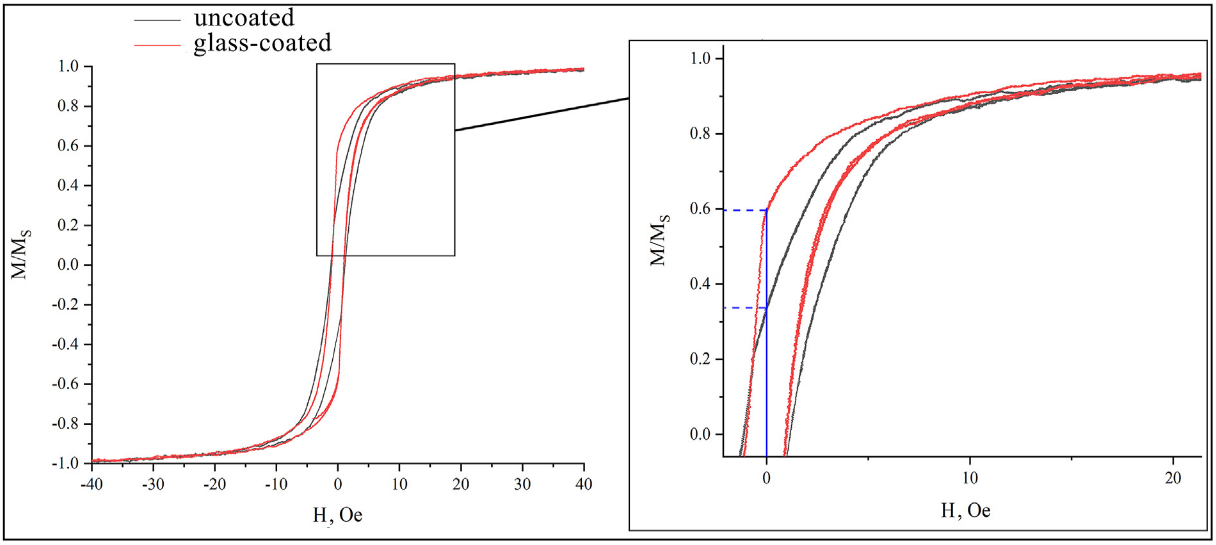

Fig. 8. Hysteresis loop of glass-coated and uncoated microwires with d/D = 0.7.

It can be seen in the insets that remanent magnetization decreases with a decrease in the d/D ratio and after glass shell removal. The values of "core" radius and thickness of a surface domain layer are evaluated. The results are presented in Table 4.

Table 4
Values of the "core" radius R_C and the thickness of a surface domain layer R_{outl}.

d/D	Presence of the glass shell	M_r/M_S	R_C/R_m	R_{outl}/R_m
0.7	Glass-coated	0.6	0.77	0.23
0.7	Uncoated	0.33	0.57	0.43
0.48	Glass-coated	0.82	0.9	0.1
0.48	Uncoated	0.34	0.58	0.42

Based on the results of Table 4, it is possible to modify the components of stress tensor in microwires with d/D = 0.7 and 0.48 by shifting the curves of stress tensor components, so that, the intersection point of radial and axial components corresponds to the experimental data.

Figs. 10 and 11 show that a lower d/D ratio (addition associated with a difference in the thermal expansion coefficients of the glass shell and amorphous metallic nucleus) leads to increase of the tensor components. Moreover, a lower initial radius of a microwire (addition associated with quenching stress) results in the same effect. This approach is approximate and allows separating correctly the regions of tensile and compressive stress to evaluate qualitatively stress distribution over microwires.

The relative position of the curves in Figs. 10 and 11 demonstrates that removal of the glass shell leads to a decrease in the stress value for the tangential and radial components of stress tensor by 100–150 MPa. Fig. 10 shows that the value of axial stress for the microwire with the highest initial stress level (d/D = 0.48) decreases by 500 MPa after glass shell removal. Fig. 11 demonstrates that the value of axial stress for the microwire with the lowest initial stress level (d/D = 0.7) decreases by 300 MPa after glass shell removal. That is, the behavior of a change in the stress tensor and, consequently, in an average value of stress in the material is different for the microwires with higher and lower d/D ratios. This should affect the change in the behavior of domain structure evolution and in magnetization reversal processes.

The effect of stress appearing in the material under

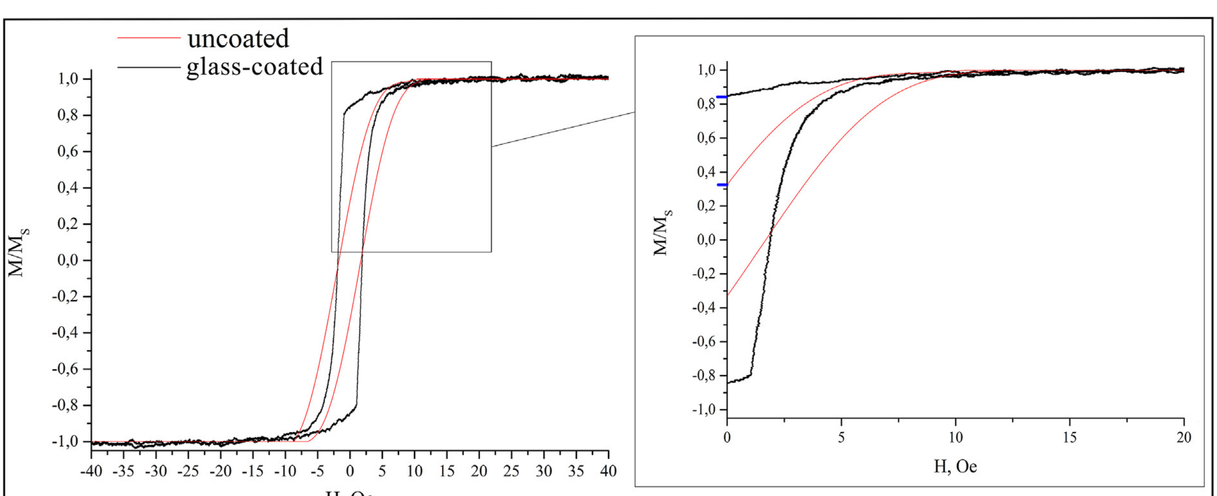

Fig. 9. Hysteresis loop of glass-coated and uncoated microwires with d/D = 0.48.

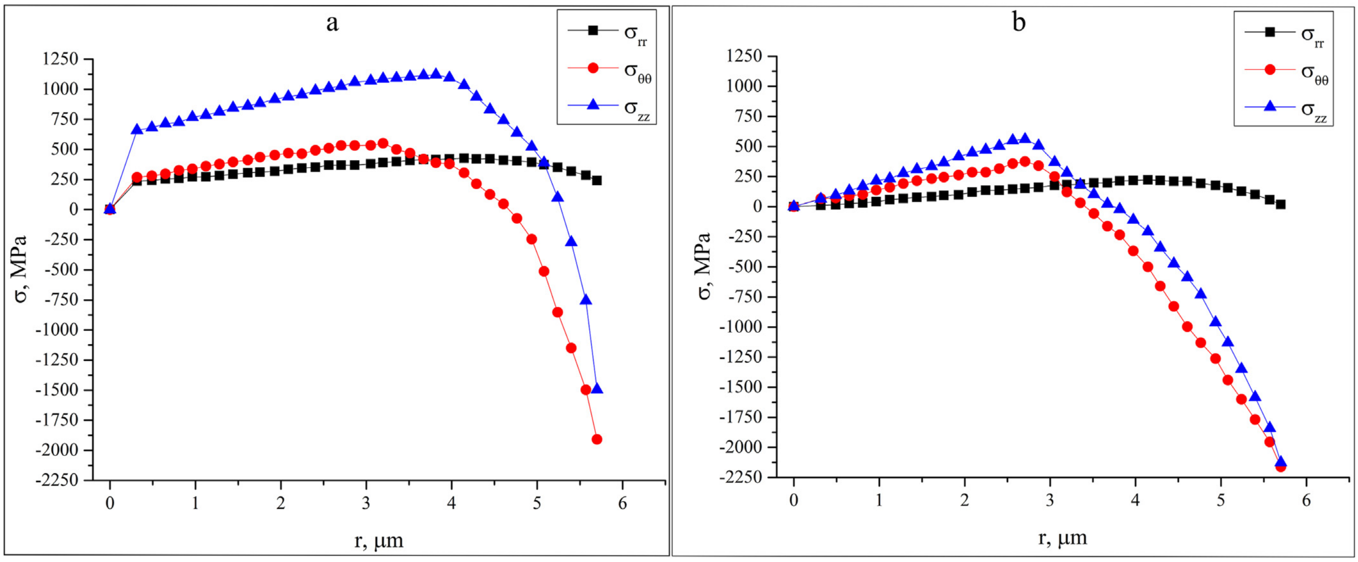

Fig. 10. Distribution of the components of internal stress tensor over the radius of the amorphous metallic nucleus for (a) glass-coated and (b) uncoated microwires with d/D = 0.48.

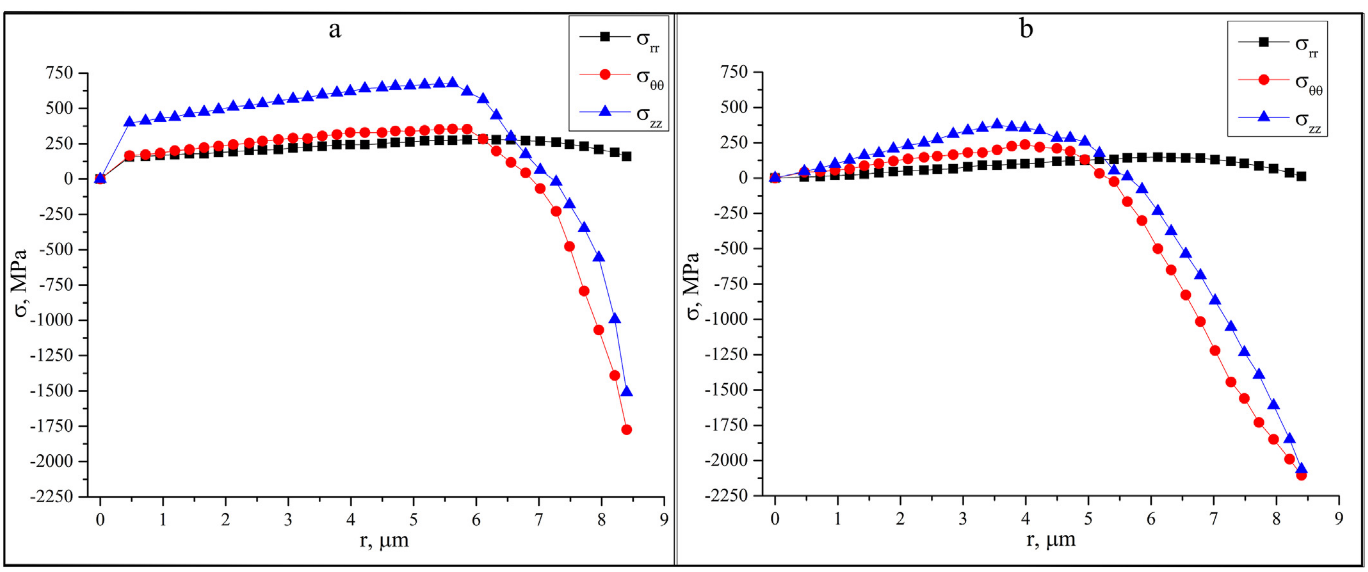

Fig. 11. Distribution of the components of internal stress tensor over the radius of the amorphous metallic nucleus for (a) glass-coated and (b) uncoated microwires with d/D = 0.7.

magnetization needs to be considered in addition to initial stress state. As mentioned earlier, amorphous microwires of $Fe_{73.8}Cu_1Nb_{2.1}B_{9.1}Si_{13}$ composition have saturation magnetostriction $\lambda_s = 39x10^{-6}$. The Young's modulus E_a is 150 GPa [30].According to the Hooke's low:

$$\sigma = \varepsilon E_a \tag{6}$$

where ε is the tensile strain of a material. The maximum tensile strain of a ferromagnetic, related to magnetization in an external magnetic field, corresponds to the value of saturation magnetostriction. One may suppose that $\lambda_s = \varepsilon$. By substituting the known values of λ_s and E_a to Eq. (6), it is possible to estimate the maximum tensile stress appearing under magnetization in a saturation magnetic field. Then σ = 6 MPa. This is substantially less than the value of an average stress in a microwire (100–200 MPa) [24]. Moreover, this value is considerably below the tension stress applied to a microwire in our experiments (100–2000 MPa).

The value of the average stress σ_a for an amorphous microwire under tension can be estimated by von Mises's classical expression for stress [30]:

$$\sigma_a = \sqrt{(\sigma_{rr} - \sigma_{\theta\theta})^2 + (\sigma_{\theta\theta} - \sigma_{zz} - \sigma_t)^2 + (\sigma_{zz} + \sigma_t - \sigma_{rr})^2 / 2} \tag{7}$$

where σ_{rr}, $\sigma_{\theta\theta}$, and σ_{zz} are the radial, tangential, and axial diagonal components of a stress tensor, respectively. These components are estimated in Ref. 29. σ_t is the addition to the axial component, related to the tension stress applied to the cross-section of the amorphous metallic nucleus of a microwire.

There are two approaches to the estimation of an average stress in a microwire. This is directly related to its composition magnetic structure. From the one hand, an average stress can be estimated over the whole bulk of a microwire. From the other hand, it is possible to divide the bulk of a microwire into two regions with

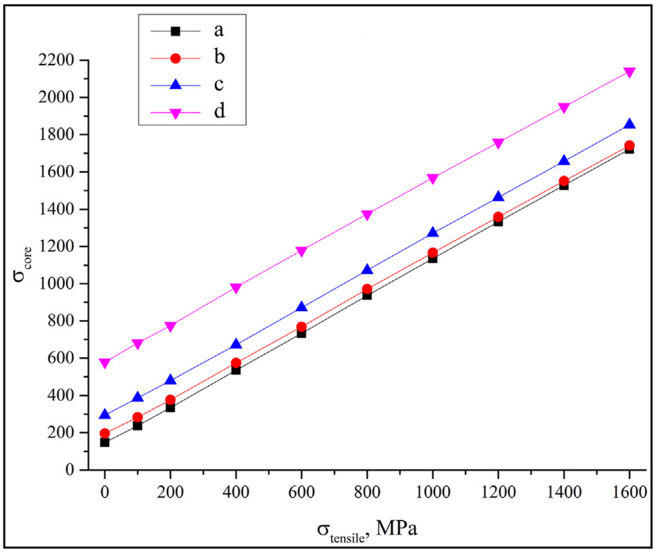

Fig. 12. Change in an average stress in the "core" under tension: (a) uncoated wire with d/D = 0.7; (b) uncoated wire with d/D = 0.48; (c) glass-coated wire with d/D = 0.7; (d) glass-coated wire with d/D = 0.48.

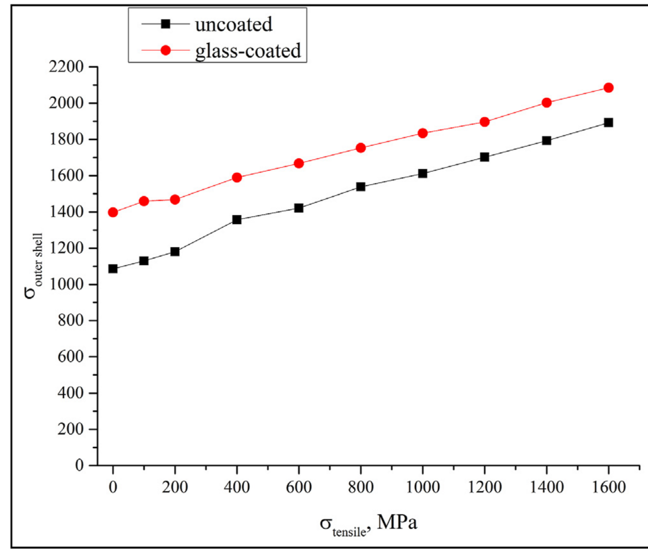

Fig. 13. Change of an average stress in a surface domain layer for the microwire with d/D = 0.48.

different character of magnetization, size of domains, and stress distribution, i.e., the "core" and surface domain layer. Figs. 10 and 11 clearly demonstrate that every component of a stress tensor is positive in the central part of the wire. In the case of a surface domain layer, axial, and tangential components of a stress tensor are predominantly negative.

Then, the calculation of an average stress in a surface domain layer and the "core" is more preferred. However, one needs to take into consideration that the applied tension stress changes the size of domain regions. It is considered by analogy with Ref. 29 that the transition from "core" domains to the domains of a surface layer occurs when the radial component of a stress tensor is equal to the axial component.

Figs. 12 and 13 show dependence of a calculated average stress (in the "core" and surface layer) on the applied tension stress σ_t.

As can be seen from Figs. 12 and 13, the curves of the dependence of an average stress in the "core" on the tension stress are described by a linear function. At that, the rate of an increase in the average stress in the "core" is roughly the same for all types of the microwires under study. A higher level of stress under tension is reached in microwires with a higher initial stress state. The value of an average stress in the surface domain layer is three times higher than that in the "core". As can be seen, the value of an average stress in the surface domain layer is increased by about 70% under tension of up to 1600 MPa. At that, the stress in the "core" is increased by 270% under the same tension stress. Table 5 demonstrates key results corresponding to the obtained dependence.

Table 5 shows that the value of an average stress in the "core" is about 150–200 MPa for uncoated microwires. An average stress in the "core" is increased for glass-coated microwires and exceeds 550 MPa for the microwire with d/D = 0.48. It follows that Eq. (2) is fulfilled for uncoated microwires under tension. However, in the case of glass-coated microwires there is a prolonged region where the value of initial stress is higher than that of the applied tension stress. In this region, coercivity changes by a more complex mechanism.

There is still a question on the relative position of the curves of coercivity dependence on the stress for glass-coated and uncoated microwires. Obviously, a higher position of the curves for uncoated microwires contradicts the dependence in Fig. 12.

Table 5
Main characteristics of the average stress dependence on the tension stress.

d/D	Domain region	Presence of the glass shell	Initial σ, MPa
0.48	Core	Glass-coated	578
		Uncoated	196
	Surface domain layer	Glass-coated	1400
		Uncoated	1086
0.7	Core	Glass-coated	294
		Uncoated	148

To resolve this contradiction, the peculiarities of the tension of glass-coated microwires should be taken into account. Following Ref. 29, the stress tensor of glass-coated microwires differs from that of uncoated microwires in positive addition to σ_{zz}, σ_{rr} and $\sigma_{\theta\theta}$ components. As already mentioned, it is related to the difference in the thermal expansion coefficients of the glass shell and amorphous metallic nucleus. The character of deformation process under tension should be taken into account because of different Poisson's ratios and Young's moduli for glass and an amorphous metal. The glass shell and amorphous metallic nucleus are deformed in a differently under the same external tension.

By analogy with Eq. (1), it can be written for the glass shell:

$$\sigma_g = F / (S_g + S_a E_a / E_g) \tag{8}$$

where σ_g is the tension stress applied to the glass shell, F is the applied force, S_a is the sectional area of the metallic nucleus, S_g is the sectional area of the glass shell, E_g and E_a are the Young's moduli of the glass and amorphous metallic nucleus, respectively. The classical expression for the Poisson's ratio is [31]:

$$\nu = E\Delta d / \sigma d \tag{9}$$

where ν is the Poisson's ratio, Δd is the change in the diameter of a wire, d is the diameter of a wire, E is the Young's modulus, σ is the applied stress. Based on Eqs. (1), (8) and (9), the expressions for a change in the diameter of the amorphous metallic nucleus and glass shell can be written as:

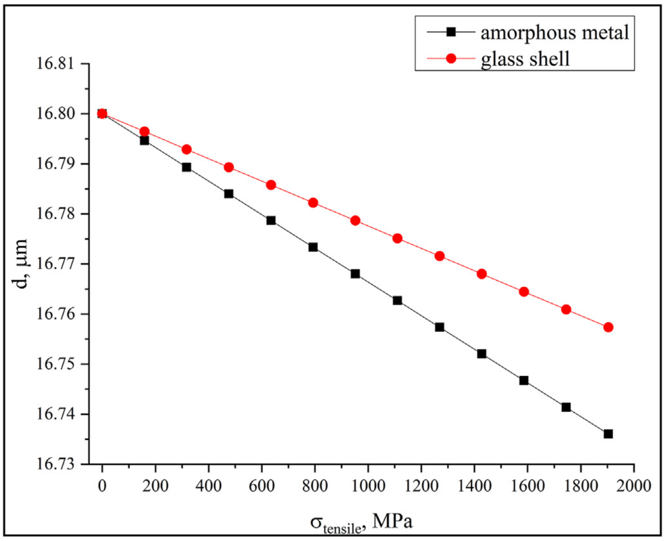

Fig. 14. Change in the diameter of the glass shell and amorphous metallic nucleus depending on the tension stress applied to the amorphous metallic nucleus.

$$\Delta d_g = (\nu_g \sigma_t / E_a) d_g \quad (10)$$

$$\Delta d_a = (\nu_a \sigma_t / E_a)\, d_a \quad (11)$$

where Δd_g and Δd_a are the changes in the diameter of the glass shell and amorphous metallic nucleus, respectively; ν_g and ν_a are the Poisson's ratios for the glass shell and amorphous metallic nucleus. The Poisson's ratio can be considered to be 0.2 for the glass shell and 0.3 for the amorphous metallic nucleus [34]. However, it is assumed there is no interaction between the glass shell and the amorphous metallic nucleus. Fig. 14 demonstrates the curves of diameter change dependence of the glass shell and amorphous metallic nucleus on the tension stress applied to the amorphous metallic nucleus for the wires with d/D = 0.7.

It becomes apparent in Fig. 14 that a decrease in the inner diameter of the glass shell is slower than that in the diameter of the amorphous core. Herewith, the change in the diameter is about hundredths of a micrometer. Considering that the materials of the amorphous core and glass shell are not perfect, there is an adhesion between these parts of a wire which prevents separation of the glass shell from the amorphous core. In this case, adhesion is a negative addition to the components of the stress tensor of the amorphous core.

As mentioned earlier, as a result of different values of the thermal expansion coefficients of the glass shell and amorphous metallic nucleus there are positive additions to the components of stress tensor. These additions lead to excess deformation of the amorphous core. Then there is gradual removal of this excess deformation with an increase in lateral deformation under tension of the amorphous metallic nucleus. As a result, there is a gradual decrease in the components of stress tensor under tension. When excess deformation is completely compensated by lateral deformation, the stress tensor of a glass-coated microwire is transformed into the stress tensor of an uncoated microwire. Herewith, there is a addition to axial components as a result of amorphous core tension. Then the curve of $H_C(\sigma)$ dependence for a glass-coated microwire is transformed to $H_C(\sigma)$ dependence of an uncoated microwire. However, adhesion prevents separation of the glass shell from the amorphous core. Therefore, the axial component of the stress tensor increases under subsequent tension, but also there is negative addition to the axial component related to adhesion. This leads to an unexpected result: the presence of adhesion brings to the average stress in an uncoated microwire being higher than that in a glass-coated wire. As a result, the curve of $H_C(\sigma)$ dependence for an uncoated microwire is higher than the same curve for a glass-coated wire. Fig. 6 clearly demonstrates this effect.

Adhesion for a glass-coated microwire was investigated in Ref. 22. The value of adhesion was 58 MPa which was lower by at least an order of magnitude than it could be expected from the results in Fig. 14. It follows that the value of adhesion may significantly vary for microwires with different geometrical parameters.

Thus, in the view of the adhesion and compensation of addition to the components of the stress tensor (which is related to different values of the thermal expansion coefficients of the glass shell and amorphous metallic nucleus), there is good agreement between the obtained experimental results (Fig. 6) and the theoretical estimation for a stress state of the "core" (Fig. 11).

4. Conclusions

The evolution of magnetic hysteresis properties under tension has been studied for microwires of $Fe_{73.8}Cu_1Nb_{2.1}B_{9.1}Si_{13}$ composition with different initial stress states.

It has been obtained that coercivity increases with an increase in the applied tension stress. Herewith:

- coercivity dependence on the stress is reversible and can consist of two parts with "linear" and "power" dependence which correlates with the initial level and distribution of stress in the material; - a decrease in the initial average stress leads to a decrease in the rate of coercivity increase; - an increase in the initial average stress leads to an increase in the "linear" region of tension.

It has been assumed that peculiarities of magnetization reversal process of glass-coated microwires are related to the adhesion between the glass shell and amorphous metallic nucleus.

Declaration of competing interest

The authors declare that they have no known competing financial interests or personal relationships that could have appeared to influence the work reported in this paper.

CRediT authorship contribution statement

O.I. Aksenov: Conceptualization, Methodology, Validation, Formal analysis, Investigation, Writing - original draft, Writing - review & editing, Visualization, Project administration, Funding acquisition. **A.A. Fuks:** Methodology, Validation, Investigation, Visualization. **A.S. Aronin:** Conceptualization, Validation, Formal analysis, Writing - review & editing, Supervision.

Acknowledgements

The research is carried out within the state task of ISSP RAS with the partial support of the RFBR (grants 18-32-00251, 16-53-48012).

References

[1] P. Corte-Leon, V. Zhukova, M. Ipatov, J.M. Blanco, J. Gonzalez, et al., Stress dependence of the magnetic properties of glass-coated amorphous microwires, J. Alloys Compd. 789 (2019) 201–208.
[2] A. Dzhumazoda, L.V. Panina, M.G. Nematov, F.S. Tabarov, A.T. Morchenko, et al., Controlling the Curie temperature in amorphous glass coated microwires by heat treatment, J. Alloys Compd. 802 (2019) 36–40.

[3] A. Zhukov, M. Ipatov, P. Corte-Leon, L. Gonzalez-Legaretta, J.M. Blanco, V. Zhukova, Soft magnetic microwires for sensor applications, J. Magn. Magn Mater. 498 (2020) 166180.
[4] J. Durand, Magnetic properties of metallic glasses, in: H. Beck, H.-J. Giintherodt (Eds.), Topics in Applied Physics. Glassy Metals II, vol. 53, Springer, New York, 1983.
[5] G. Herzer, Amorphous and nanocrystalline materials, in: Encyclopedia of Materials: Science and Technology, Elsevier Science Ltd, 2001, pp. 149–157.
[6] N.N. Orlova, A.S. Aronin, S.I. Bozhko, Y.P. Kabanov, V.S. Gornakov, Magnetic structure and magnetization process of the glass-coated Fe-based amorphous microwire, J. Appl. Phys. 111 (2012), 073906.
[7] O.I. Aksenov, G.E. Abrosimova, A.S. Aronin, N.N. Orlova, et al., The change of domain structure of the amorphous microwire of $Fe_{73.5}Cu_1Nb_3Si_{13.5}B_9$ composition under thermal treatment, J. Appl. Phys. 122 (2017) 235103.
[8] N.N. Orlova, V.S. Gornakov, A.S. Aronin, Role of internal stresses in the formation of magnetic structure and magnetic properties of iron-based glass coated microwires, J. Appl. Phys. 121 (2017) 205108.
[9] C. Garcia, A. Zhukov, J. Gonzalez, V. Zhukova, R. Varga, J.J. del Val, V. Larin, J.M. Blanco, Studies of structural and magnetic properties of glass-coated nanocrystalline $Fe_{79}Hf_7B_{12}Si_2$ microwires, J. Alloys Compd. (2006) 116–119.
[10] V. Larin, V. Zhukova, A. Zhukov, A. Torcunov, M. Vazquez, Tailoring of magnetic anisotropy in Fe-rich glass-coated magnetic microwires by thermo-mechanical annealing, Sens. Actuators, A 106 (2003) 96–100.
[11] A. Zhukov, A. Talaat, M. Ipatov, J.M. Blanco, V. Zhukova, Tailoring of magnetic properties and GMI effect of Co-rich amorphous microwires by heat treatment, J. Alloys Compd. 615 (2014) 610–615.
[12] M. Vazquez, H. Chiriac, A. Zhukov, L. Panina, T. Uchiyama, On the state-of-the-art in magnetic microwires and expected trends for scientific and technological studies, Phys. Status Solidi A 208 (2011) 493–501.
[13] A. Zhukov, Design of the magnetic properties of Fe-rich, glass-coated microwires for technical applications, Adv. Funct. Mater. 16 (2006) 675–680.
[14] R. Varga, A. Zhukov, J.M. Blanco, M. Ipatov, V. Zhukova, J. Gonzalez, P. Vojtaník, Fast magnetic domain wall in magnetic microwires, Phys. Rev. B 74 (2006) 212405.
[15] A. Zhukov, J.M. Blanco, M. Ipatov, A. Chizhik, V. Zhukova, Manipulation of domain wall dynamics in amorphous microwires through the magnetoelastic anisotropy, Nanoscale Res. Lett. 7 (2012) 223.
[16] K.R. Pirota, L. Kraus, H. Chiriac, M. Knobel, Magnetic properties and giant magnetoimpedance in a CoFeSiB glass-covered microwire, J. Magn. Magn Mater. 221 (2000) L243–L247.
[17] A. Talaat, V. Zhukova, M. Ipatov, J.M. Blanco, L. Gonzalez-Legarreta, B. Hernando, J.J. del Val, J. Gonzalez, A. Zhukov, Optimization of the giant magnetoimpedance effect of Finemet-type microwires through the nano-crystallization, J. Appl. Phys. 115 (2014) 17A313.
[18] J.M. Blanco, A. Zhukov, J. Gonzalez, Torsional stress impedance and magneto-impedance in $(Co_{0.95}Fe_{0.05})_{72.5}$ $Si_{12.5}B_{15}$ amorphous wire with helical induced anisotropy, J. Phys. D Appl. Phys. 32 (1999) 3140–3145.
[19] H. Chiriac, T.-A. Ovari, A. Zhukov, Magnetoelastic anisotropy of amorphous microwires, J. Magn. Magn Mater. 254–255 (2003) 469–471.
[20] P. Aragoneses, J.M. Blanco, L. Dominguez, J. Gonzalez, A. Zhukov, M. Vazquez, The stress dependence of the switching field in glass-coated amorphous microwires, J. Phys. D Appl. Phys. 31 (1998) 3040–3045.
[21] A. Zhukov, A.F. Cobeno, J. Gonzalez, J.M. Blanco, P. Aragoneses, L. Dominguez, Magnetoelastic sensor of liquid level based on magnetoelastic properties of Co-rich microwires, Sensor. Actuator. A 81 (2000) 129–133.
[22] M. Churyukanova, S. Kaloshkin, E. Shuvaeva, A. Stepashkin, et al., Non-contact method for stress monitoring based on stress dependence of magnetic properties of Fe-based microwires, J. Alloys Compd. 748 (2018) 199.
[23] P. Corte-Leon, V. Zhukova, M. Ipatov, J.M. Blanco, J. Gonzalez, M. Churyukanova, J.M. Baraibar, S. Taskaev, A. Zhukov, Stress dependence of the magnetic properties of glass-coated amorphous microwires, J. Alloys Compd. 789 (2019) 201–208.
[24] H. Chiriac, T.A. Ovari, G. Pop, Internal stress distribution in glass-covered amorphous magnetic wires, Phys. Rev. B 52 (1995) 10104.
[25] A. Sypien, J. Kusinski, The structure and mechanical properties of amorphous and nanocrystalline Fe–Si–B alloys, J. Microsc. 224 (2006) 111–113.
[26] O.I. Aksenov, N.N. Orlova, A.S. Aronin, The method of hysteresis properties measurement for magnetic microwires under stretching in situ, Instrum. Exp. Tech. 62 (2019) 723–725.
[27] E.Ia Badinter, E.M. Lysko, Microwire and Resistivity Devices, Shtinitsa, Kishinev, 1962, pp. 52–62.
[28] H. Chiriac, T.A. Ovari, Gh. Pop, Magnetic behavior of glass-covered amorphous wires, J. Magn. Magn. Mater 157-158 (1996) 227–228.
[29] M. Vazquez, D.-X. Chen, The magnetization reversal process in amorphous wires, IEEE Trans. Magn. 31 (1995) 1229–1238.
[30] R.M. Jones, Deformation Theory of Plasticity, Bull Ridge Corporation, Blacksburg, Virginia, 2009.
[31] G.P. Johari, On Poisson's ratio of glass and liquid vitrification characteristics, Phil. Mag. 86 (2006) 1567–1579.